JOURNAL OF GEOPHYSICAL RESEARCH, VOL. 92, NO. C2, PAGES 1527–1544, FEBRUARY 15, 1987

Large-Scale Structure of the Spring Transition in the Coastal Ocean off Western North America

P. TED STRUB, J. S. ALLEN, A. HUYER, AND R. L. SMITH

College of Oceanography, Oregon State University, Corvallis

Past measurements off the coast of central Oregon and Washington have shown that the rapid change from northward monthly mean winter winds to southward summer winds forces a "spring transition" of the coastal ocean: sea levels and temperatures drop, and mean surface currents shift from northward to southward. Current and water temperature data from 35°N to 48°N from 1981 and 1982, and sea level and wind stress data from 1971–1975 and 1980–1983, show the transition to have a large alongshore scale, typically 500 to 2000 km; the large-scale wind stress appears to be the forcing mechanism at latitudes north of approximately 37°N. South of 37°N, sea level usually falls more gradually before the northern transition event. Both wind and sea level events generally progress from south to north over a 3- to 10-day period, but this is not always true. Several aspects of the spring transition reflect coastal trapped wave dynamics. Previous studies at 45°N found persistent vertical shear of the southward summer current, associated with a cross-shelf density gradient. During 1982 the shear and the density front develop over the shelf break immediately after the transition at 43°N and to the south, but they are much less persistent than at 48°N. The stronger winds between 38°N and 42°N and the narrower shelf result in an offshore displacement of the density front and vertical shear past the shelf break, leaving the water over the shelf less stratified and more subject to barotropic reversals of the current than that farther north, where the front stays closer to the coast.

INTRODUCTION AND BACKGROUND

Off the west coast of North America the transition from winter to summer wind regimes occurs as the Aleutian low-pressure system weakens and moves northwestward and the North Pacific high-pressure system strengthens and moves to the north, resulting in southward winds along the west coast of North America [*Huyer*, 1983]. Off central Oregon the response of the coastal ocean to this large-scale change in winds is quite rapid, as is documented in detail by *Huyer et al.* [1979]. At 45°N in 1973 and 1975 the winter regime in the coastal ocean consisted of high sea levels, monthly mean northward flow over the shelf, little monthly mean vertical shear in the alongshore current, correspondingly small cross-shelf density gradients, and large baroclinic fluctuations in alongshore velocity with periods less than a month; the summer regime consisted of low sea levels and southward monthly mean surface flow over a northward (or weaker southward) undercurrent, resulting in substantial monthly mean vertical shear, with a strong mean cross-shelf density gradient. The fluctuations with periods less than a month in summer were mostly barotropic and weaker than in the winter [*Kundu et al.*, 1975; *Huyer et al.*, 1978]. The transition between winter and summer regimes occurred within approximately 1 week; the sea level and currents changed most rapidly followed by the establishment of the baroclinic shear and cross-shelf density gradient over a 5- to 10-day period. *Huyer et al.* [1979] conclude that the coastal ocean transition is controlled by the local southward winds, which cause southward alongshore surface flow and offshore surface Ekman transport. This draws denser water onto the sloping shelf and establishes the cross-shelf density gradient, which is associated with the vertical shear of the alongshore current through the thermal wind relation. At 45°N in 1972, 1973, and 1975 the summer regime of low sea level and southward midshelf surface currents (down to 40 m) was more persistent than the southward winds; i.e., sea levels remained low, and currents usually remained southward even during northward wind events from late March to late July [*Kundu et al.*, 1975; *Huyer et al.*, 1979].

Recently, data collected from 35°N to 48°N have been used to examine the north-south differences in the seasonal cycles

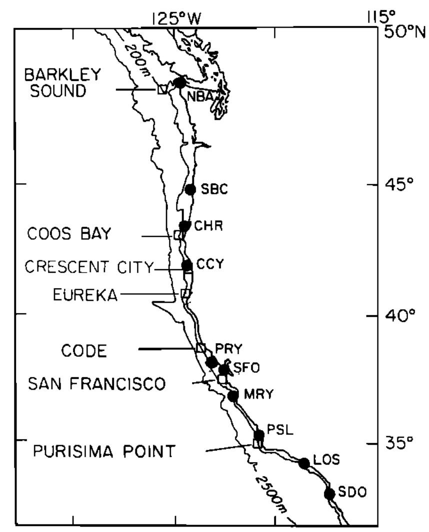

Fig. 1. Locations of current meter moorings (open squares) and sea level stations (solid circles). Sea level stations are (north to south) Neah Bay (NBA; 48.4°N), South Beach (SBC; 44.6°N), Charleston (CHR; 43.3°N), Crescent City (CCY; 41.8°N), Point Reyes (PRY; 38.0°N), San Francisco (SFO; 37.8°N), Monterey (MRY; 36.6°N), Port San Luis (PSL; 35.2°N), Los Angeles (LOS; 33.7°N), and San Diego (SDO; 32.8°N). Current meter mooring locations are Barkley Sound (so named since it as the most offshore mooring on a line off Barkley Sound, though it is some distance from Barkley sound), British Columbia, Canada (48.3°N), Coos Bay, Oregon (43.1°N), Crescent City, California (41.9°N), Eureka, California (40.9°N), Coastal Ocean Dynamics Experiment (CODE) (38.6°N), San Francisco, California (37.4°N), and Purisima Point, California (34.7°N).

Paper number 6C0502.
0148-0227/87/006C-0502$05.00

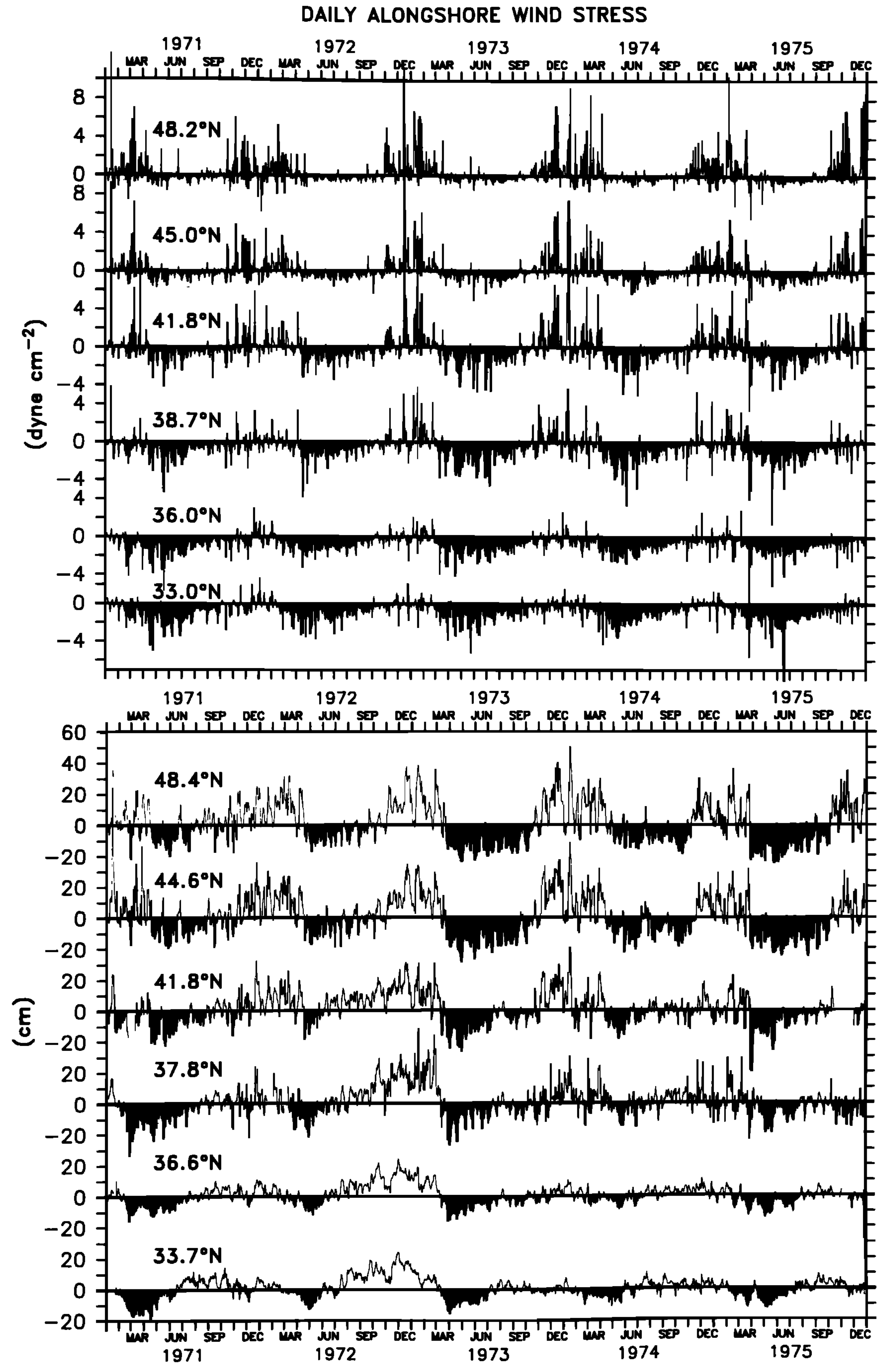

Fig. 2. (top) Alongshore wind stress, derived from 6-hourly pressure fields, and (bottom) sea level, after the removal of the mean values and long-term trends determined from 9 to 34 years of monthly data for (left) 1971–1975 and (right) 1980–1983.

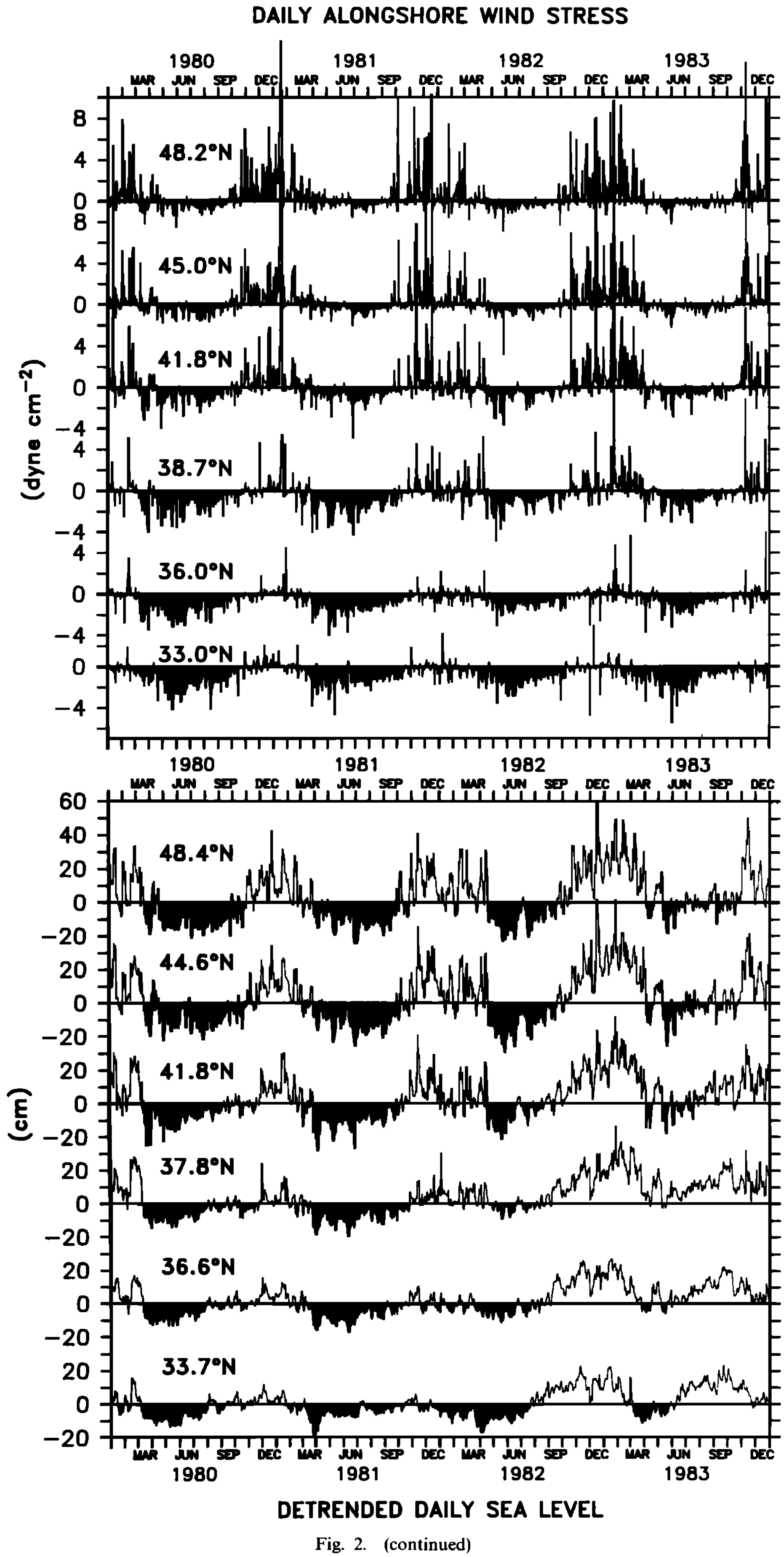

Fig. 2. (continued)

of coastal wind stress, sea level, currents, and temperatures (*Strub et al.* [this issue], hereinafter referred to as SAHSB). In the present paper the same data are used to look at the large-scale structure of the transition event and the first few months of the summer regime. For the purposes of this paper the spring transition is defined as a large-scale change from the winter to the summer regimes, as is indicated by the rapid lowering of sea level, the switch to southward surface currents with a mean vertical shear that is more persistent than the several-day fluctuations in alongshore wind stress and currents, and the upwelling of cold water that results in a persistent cross-shelf temperature difference. Since sea level and wind stress data are available for 9 years and current and temperature data are availabe for only 2, coastal sea level is used as the primary indicator of the transition. The date of the transition is taken to be the time that sea level drops rapidly, over a several-day period, and stays low at 41.8°N, a location where the event is seen clearly in the sea level on most years; for the 9 years examined, the dates of the transition in sea level at 41.8°N ranged from March 22 to April 18.

Questions about the large-scale nature of the spring transition include the following:

1. What is the alongshore scale of the event as is seen in sea level, current, and water temperature observations, and how is that scale related to the scale of the wind forcing?
2. Is the persistence in coastal response greater than in the wind forcing, as was seen at 45°N previously?
3. Is the sequence of events that define the transition similar everywhere along the coast, i.e., the temporal relation between the onset or strengthening of southward wind stress, the drop in sea level, the upwelling of colder water and development of the cross-shelf temperature difference, and the develpment of the southward current and baroclinic shear?
4. Is the coastal ocean's preference for poleward propagation important or necessary in driving the event, or can the event progress equatorward as easily as poleward?

DATA SETS

The data used to examine the large-scale alongshore structure of the spring transition consist of low-passed ($\omega < 0.5$ cpd) wind stress, sea level, current, and temperature records. The locations of the tide gages and moorings are seen in Figure 1, and all the data are more completely described by SAHSB, *Winant and Bratkovich* [1983], *Brown et al.* [1983], *Halliwell and Allen* [1983], *Denbo et al.* [1984], *Winant et al.* [1985], *Irish* [1985], *Halliwell and Allen* [1985], and *Thomson et al.* [1985].

Nine years (1971–1975 and 1980–1983) of wind stress and sea level data were available for analysis and are used in this study. The wind stresses were calculated from wind velocities derived from 6-hourly surface pressures on a 3° grid [*Bakun*, 1973], using bulk formula [*Large and Pond*, 1981] at 10 coastal locations between 33°N and 48°N. The 180-km coastal separation of the locations is much less than the decorrelation length scales for these winds found by *Halliwell and Allen* [this issue], who also report high levels of statistical agreement between these pressure-derived winds and measured winds from coastal locations. Comparisons of the pressure-derived and measured winds during the 1981–1983 spring transitions indicate that the pressure-derived winds accurately reproduce the large-scale features of the wind forcing during these events. Use of these winds avoids problems encountered with measured winds, such as poor exposure and data gaps, and allows comparison of the 1981 and 1982 events to events in other years when measured winds are not available. The sea levels come from tide gages at sites with longer historical records that were used to detrend the data. Six such sites are available for 1971–1975, and 10 are available for 1980–1983 (Figure 1). The atmospheric pressure has been added to the sea level height measurements to form a subsurface pressure; the result is referred to simply as sea level. Current and temperature data are available from moorings at midshelf (near the 90-m isobath) and/or the shelf break (130-m to 155-m isobath) between 35°N and 43°N (Figure 1), with nominal sensor depths of 35 m, 70 m, and 110 m. AT 48°N the data are from 50 m, 100 m, and 150 m on a shelf break mooring over the 210-m isobath that is much farther from shore than the other moorings (Figure 1 of SAHSB). Currents and wind stresses have been projected onto their principal axes, and the major axis component is referred to as the "alongshore" component. For the 1981 and 1982 events, "limited fine mesh" (LFM) wind fields, computed by the National Weather Service from surface pressure fields with grid spacing of 190.5 km, were obtained from Dynalysis of Princeton [*Blumberg et al.*, 1984].

The mooring data from 1981 sampled the transition event (judged to be March 25–28 from the sea level data) at three locations (48°N, 42°N, and 35°N). Data from 39°N began in early April, data from 43°N and 37°N began in late April, and the 42°N mooring failed in mid-April. Thus we have three widely spaced moorings at the time of the event and five moorings during most of the summer. In 1982 we have data from moorings at six locations (48°N, 43°N, 41°N, 39°N, 37°N, and 35°N) at the time of the event (April 15–20) and during the summer, though periods of missing data occur. At 35°N, 39°N, and 43°N, data from both midshelf and shelf break moorings are available in 1982; at the other locations, data are available from only a midshelf mooring (shelf break at 48°N).

RESULTS

Figure 2 shows the wind stress and sea level data at six locations for the 9 years of data at locations between 34°N and 48°N. The mean values and long-term trends determined from 9–34 years of monthly data have been removed from the sea level shown here and elsewhere. The spring transition can be seen as the large-scale drop in sea level which generally occurs in March or April. At 38°N and to the north, variability of the sea level with periods less than a month is reduced after the transition; i.e., the low sea levels are more persistent in summer than the high sea levels are in winter. This can be seen in the monthly standard deviations of the 6-hourly sea level measurements presented in Figure 16 of SAHSB. The length of the low sea level summer regime is greater in the north than in the south, and the transition is most abrupt in the middle latitudes, 38°–45°N, justifying the use of the time of the sea level transition at 41.8°N to define the date of the overall transition. The transition can also be seen in the switch from northward to southward wind stress; north of 38°N, the variability of the wind stress with periods less than a month is greater in the winter than in the summer, as it is in sea level (Figure 16 of SAHSB). The short-term variability is relatively greater for wind stress than for sea level, making it difficult to choose the exact date of the transition on the basis of the wind alone. The summer southward wind regime lasts longer in the

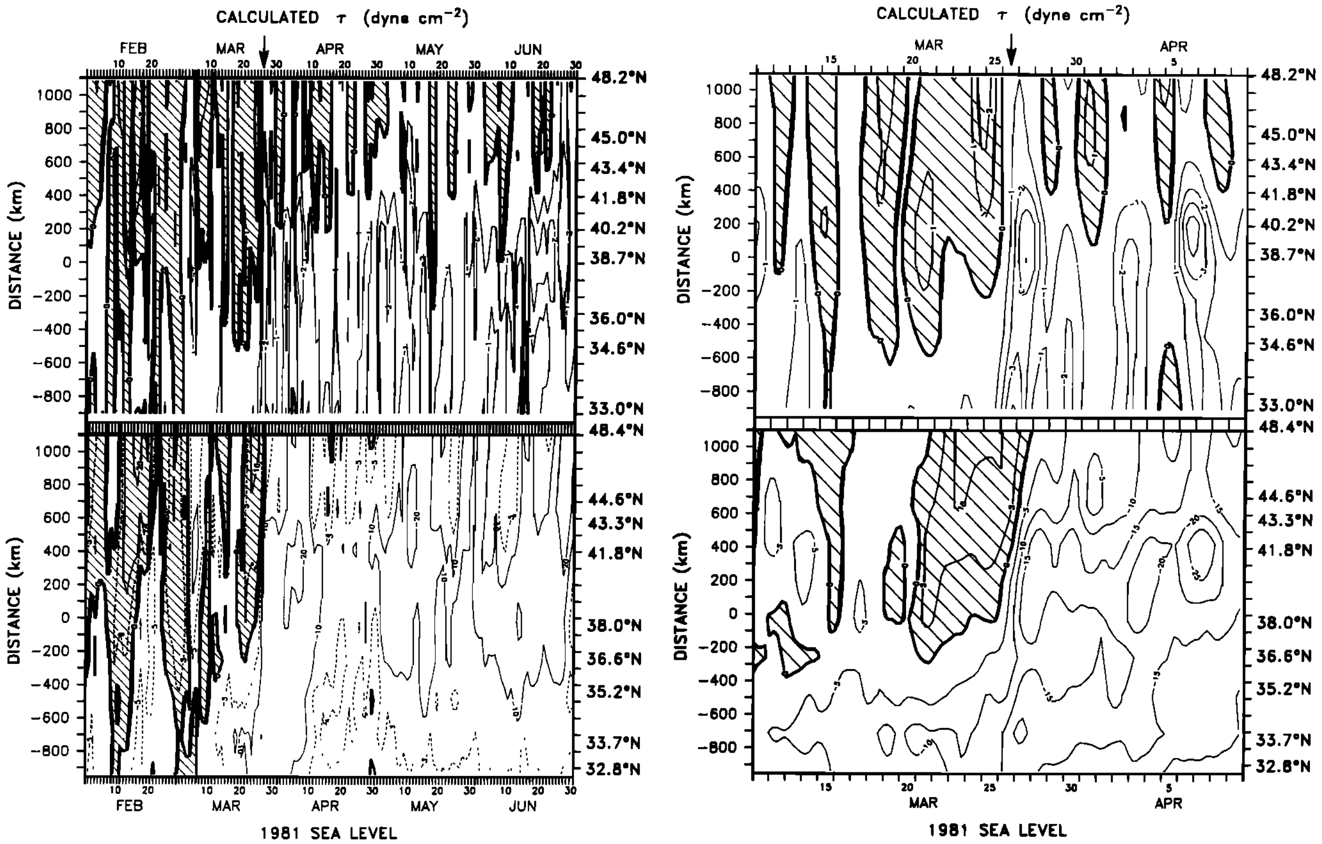

Fig. 3. Contours of (top) alongshore calculated wind stress and (bottom) adjusted sea level. Station locations are indicated by the latitudes on the right axes. (left) February–June 1981; contour intervals are 1 dyn cm^{-2} and 10 cm (with an additional dashed 5-cm contour included); areas of positive values are indicated by hatching. (right) One month centered around the transition: contour interval are 1 dyn cm^{-2} and 5 cm; areas of positive values are indicated by hatching. The nominal date determined for the transition (March 26) is indicated by the arrow at the top of each panel.

south than in the north, opposite to the pattern seen in the sea level. The magnitude of the wind reversal is greatest in the middle latitudes, 39°–42°N, similar to the sea level.

Interannual differences can be seen in the abruptness of the transition, in north-south timing and the alongshore scale of the transition, and in the length of the summer regime. At 45°N the low sea level values of the summer regimes are most persistent in years 1973 and 1975, the years of the long historical current meter records used by *Huyer et al.* [1979] in their discussion of the transition. The current and temperature data used in this study come from 1981 and 1982. During 1981, summer sea levels appear similar to the persistently low 1973 and 1975 records, while the 1982 summer data appear less persistently low. The high winter sea levels associated with the 1972–1973 and 1982–1983 El Niños can be seen in the data, especially at 38°N and to the south. The transition and summer regimes following the two El Niños are quite different, however. The 1973 transition was large-scale, and the low sea level persists through the summer, whereas the 1983 transition was weak, and the low sea levels were short lived, though winds remained primarily southward. The reason for the difference in behaviors is not known.

1981 and 1982 Spring Transitions

Alongshore Structure

Figure 3 shows contours of sea level and alongshore wind stress, over the domain from 33°N to 48°N, for the February–June period of 1981 and an expanded view of the period from March 10 to April 9. On this year the date of the transition at 41.8°N was March 26. Figure 3 shows this as the 16th day of a 30-day period, a plotting procedure followed for the other 8 years in Figures 5 and 16*a*–16*g*. The alongshore distance in these figures is measured along a smoothed coastline [*Halliwell and Allen*, 1983, 1985] and thus is longer than indicated by the latitudes alone. In Figure 3 the fluctuating winds of February and March include a period of southward wind stress of 1–2 dyn cm^{-2} for several days around February 20 (35°–41°N) and a more extensive one around March 5 (34°–43°N). These wind events temporarily lower sea levels to 5 and 10 cm below the mean, respectively. Between March 10 and 25 the winds north of 35°N continue to alternate between northward and southward, with extremes of ± 2 dyn cm^{-2} (Figure 3); sea level fluctuates in response to the wind, with values of ± 10 cm around the mean. South of 35°N, winds remain weakly southward (except for a brief reversal on March 14), and sea level slowly lowers to 10 cm below the mean. The final transition at 41.8°N comes during a wind event on March 26–38 that lowers sea levels over a large (approximately 1500 km) domain from 33°N to 44°N, with a slower and weaker response in the far north.

The winds fields from the time around the transition are presented in Figure 4, which shows LFM wind fields [*Blumberg et al.*, 1984] for the region between 30°–42°N and 117°–129°W for March 24–27. These indicate a diverging wind field, characteristic of the high pressure in the south and the low

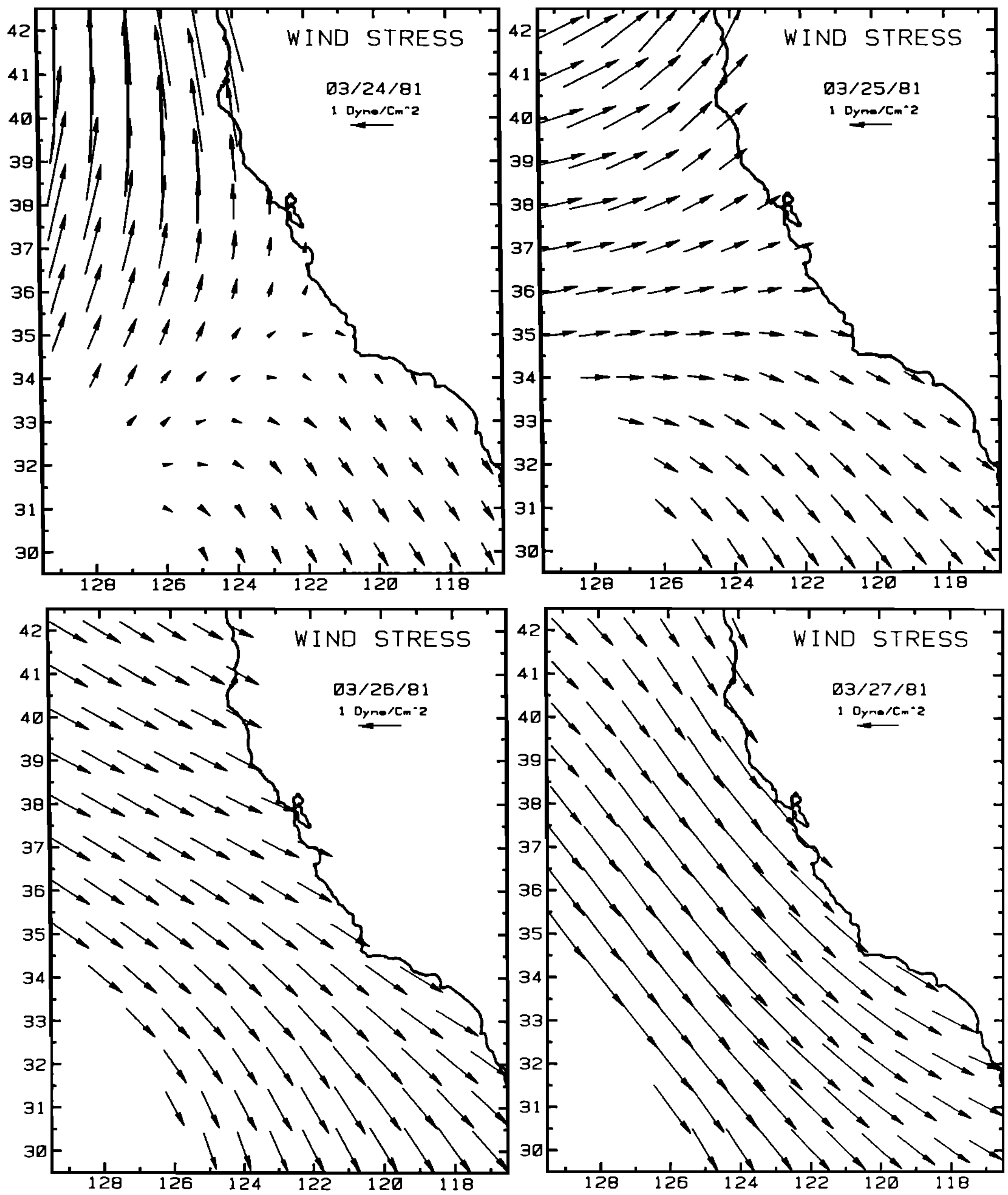

Fig. 4. Limited fine mesh (LFM) wind stress fields for March 24–27, 1981, from 30°N to 42°N, from *Blumberg et al.* [1984].

pressure in the north. Daily surface weather charts show a low-pressure system passing through the northern part of the domain on March 24–25, followed by a northward spread of the high over the entire coastal region from Canada to Baja California, while the low-pressure system stays over the western United States for several days. This high remains offshore most of the time for the next several months, though low-pressure systems do pass through the northern end of the domain. The result is the summer regime of alternating winds in the north and southward winds with fluctuating magnitude in the middle and southern domain, as is seen in Figure 3.

The LFM wind fields during the earlier southward wind event on February 15–20 initially resembled those of Figure 3 but were weaker and ended on February 22 when the high-pressure system moved onshore to a location over Nevada and Utah, a common position for high pressure in winter. The LFM wind fields during early March were different, with cyclonic curvature and winds that were southward in the north and mostly onshore in the south between 30°–35°N. These southward winds were caused by the western edge of a low-pressure system which remained over the western United States for several days, then moved southeastward. In the south, increasing high pressure over the ocean and low pressure over land kept winds there weakly southward from early March on, while storm systems continued to pass through the middle and north of the domain. The transition event involves the last low to cause northward winds in the middle of the coastal domain, followed by the rapid spread of the high-pressure system while the low remains over a large region of the western continent, creating a several-day period of strongly southward winds over the large-scale coastal domain.

After the transition in late March, maximum southward

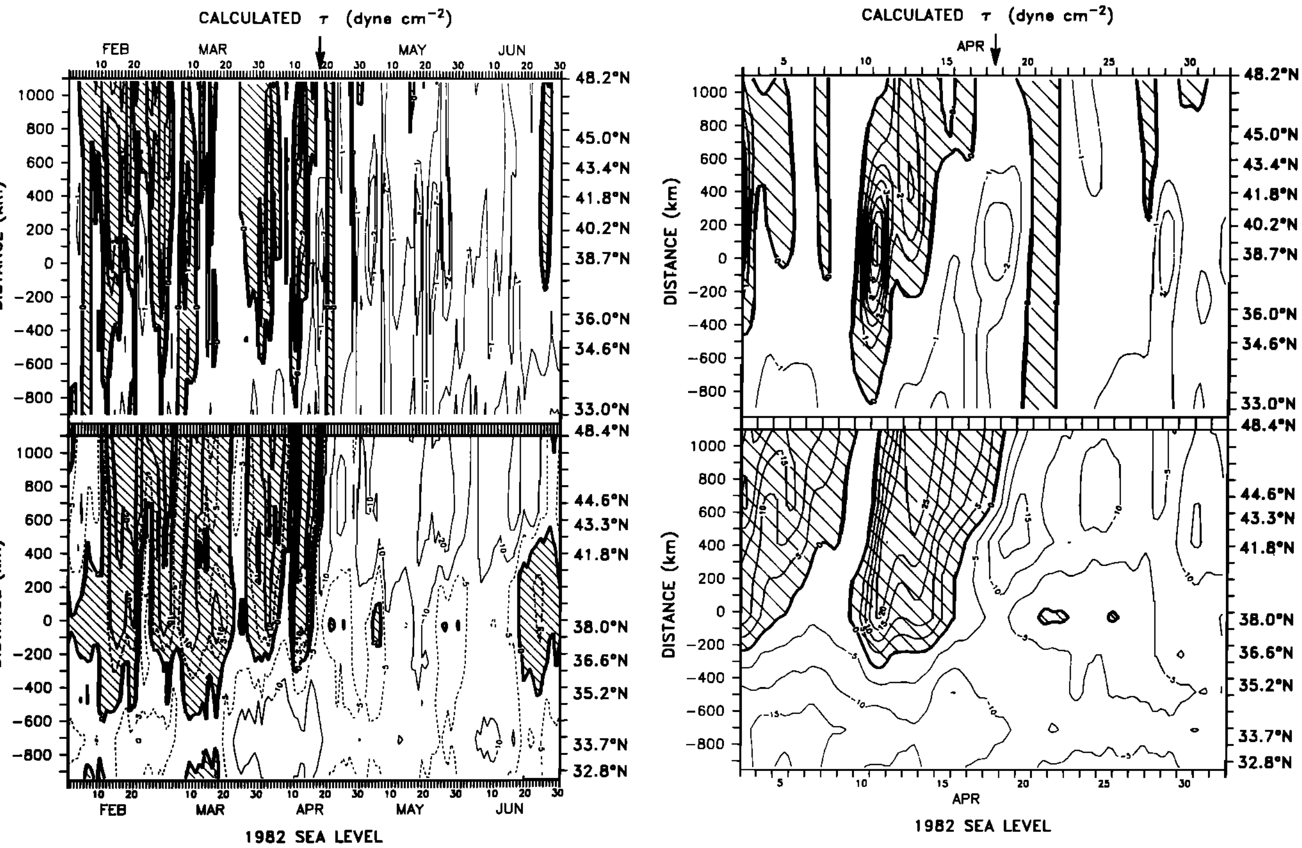

Fig. 5. Contours of alongshore calculated wind stress and sea level, as is in Figure 3, except that the right-hand panel covers the period April 3 to May 2, 1982, centered on the April 18 transition.

stresses of 2 dyn cm^{-2} usually occur south of 41°N, while maximum depressions of sea levels occur farther north (Figure 3). At 45°N the wind alternates between southward and northward, while the sea level stays low, as is reported for spring and summer 1973 by *Huyer et al.* [1979]. *Halliwell and Allen* [1984] and *Allen and Denbo* [1984] have shown both observationally and theoretically that sea levels and currents at a location over the continental shelf respond to winds that are 100 to 400 km south of that location. Thus the persistence of the low sea levels (and southward currents) seen at 45°N is consistent with the persistently southward winds integrated over some distance south of 45°N.

Figure 5 shows contours of alongshore wind stress and sea level for 1982. The transition date for this year is April 18. Again, there were southward wind events during the February–April period before the transition, specifically around February 20 and March 10–25 (Figure 5). North of 35°N, these were followed by northward events that were stronger than those in 1981. Sea levels south of 35°N dropped slowly during the light, mostly southward winds of March, as they did in 1981. A longer period elapsed in 1982 between the lowering of sea levels south of 35°N in March and the northern wind event that accompanied the seasonal strengthening of the high-pressure system in mid-April. By the time this occurred, the short, low sea level period was nearly over in the south, and the drop to -10 cm was only seen north of 39°N (Figure 5). The LFM wind fields during the 1982 transition period were very similar to Figure 4, except that the movement of the area of southward winds to the north was only half as fast. Surface pressure maps show a low-pressure system passing slowly through the region between April 10 and 15, followed by an enlargement of the high-pressure region along the coast, as occurred in 1981. The picture afterward is more confusing than that in 1981: the high moved onshore, causing the light northward winds around April 20, but reestablished itself offshore after a couple of days, where it stayed farther north than it did in 1981. Figure 5 shows that the strongest (2 dyn cm^{-2}) May and June southward wind stresses were north of 38°N in 1982, as were the regions of lowest sea levels. South of the region of maximum wind stress, the sea level at 38°N rose above its mean value several times, and the low sea level summer regime south of 38°N was less persistent than in 1981. In the north (45°–48°N), however, there were fewer periods of wind reversal, and the summer regime was stronger and more persistent that that in 1981, at least through June.

Figure 6 (top left panel) shows contours of the alongshore current for February–June 1982 from the upper current meter (35–40 m deep) over midshelf (data from 48°N come from 50 m deep over the shelf break). Figure 6 (top of right panel) shows an expanded view covering April 3 to May 2. These figures illustrate that the summer regime consists of persistently southward currents only at the 50-m shelf break location at 48°N. *Freeland et al.* [1984] show that nearby midshelf monthly mean currents from 48°N are weakly northward in summer, indicating that the data shown here from 48°N are characteristic only of the shelf break. At 39°N, current reversals resume shortly after the April 15–20 transition event, as is documented in detail by *Lentz* [this issue]. South of

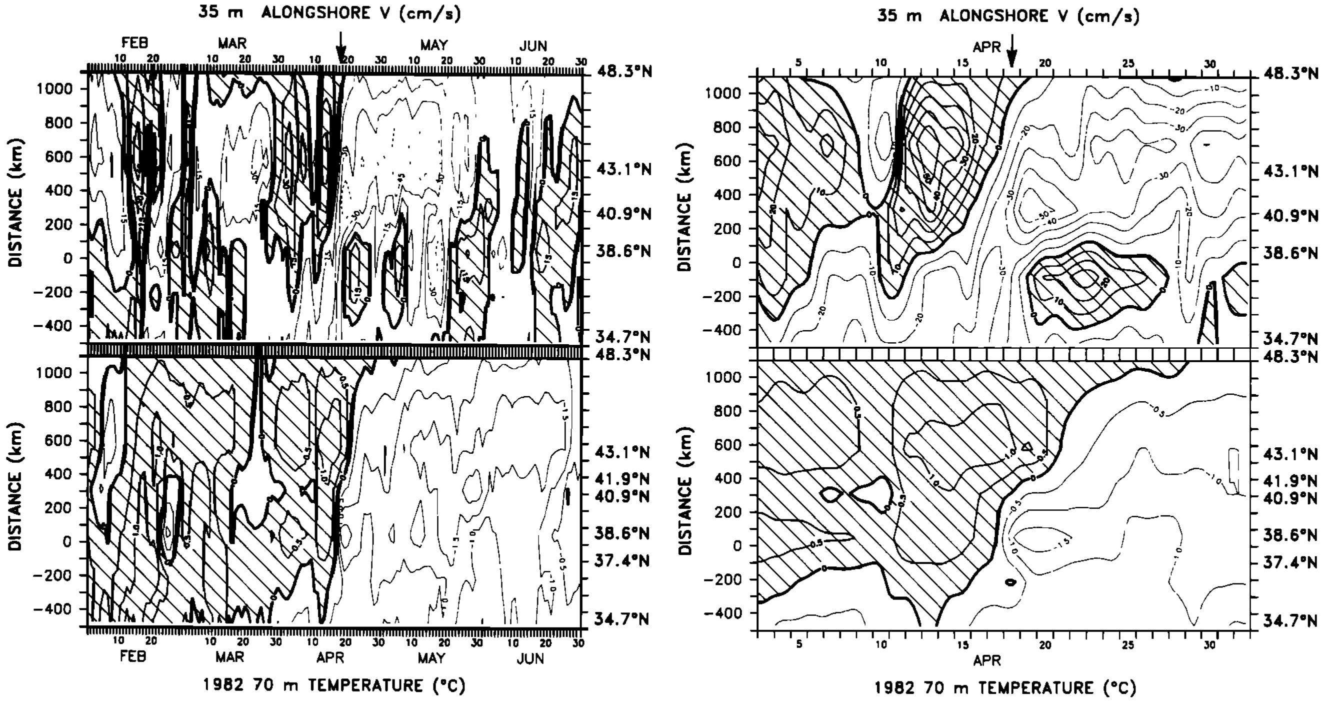

Fig. 6. Contours of (top) alongshore current from the upper (35–40 m) current meter at each midshelf mooring (except at 48°N, where the meter is 50 m deep over the shelf break) and (bottom) temperature from the lower (65–70 m) midshelf temperature sensor (except at 48°N, where the meter is 150 m deep in 210 m of water). Mooring locations are indicated by the latitudes on the right. Areas of positive values are indicated by hatching. (left) Values for February–June, 1982; (right) values for April 3 to May 2.

43°N, fluctuating midshelf currents are typical of the 1982 summer regime, rather than atypical. Data from after the 1981 transition [SAHSB, Figure 10] also show fluctuating currents at 43°N and to the south in that year. Thus current reversals are seen from 35°N to 43°N whether sea levels remain low (1981) or not (1982).

Huyer et al. [1979] suggest that the spring transition event occurs at a given location when the local winds cause enough offshore Ekman transport to draw dense water over the shelf from deeper and farther offshore and set up the cross-shelf density gradient. Though we do not have salinity measurements, the temperature records serve as an indicator of density variations. Figure 6 (bottom) presents contours of the 1982 temperature data from the lower (65–70 m) instrument over midshelf (150 m over the shelf break at 48°N). The annual means from the harmonic fits found in SAHSB have been removed from the records before contouring. Periods of southward winds (February 5 and 20 and March 10–15) before the transition event result in water temperatures that become slightly cooler (0.5°C) than the annual mean. The transition event is characterized by a dramatic, large-scale 1°–2°C drop in temperature. The most persistent characteristic of the summer regime seems to be the presence of cold water over the shelf.

Figures 6 and 5 show that alongshore velocity and sea level respond rapidly to the wind stress in like manners. After the transition, periods of northward currents correspond to rises in sea level, while temperatures remain low. This is generally true of the entire April–June period in 1982 (northward currents in Figure 6 correspond to periods of higher sea level in Figure 5). Figures 5 and 6 show that the temperature drop at 70 m lags the wind, alongshore current, and sea level by 3–5 days, with the largest lag observed in the north. This temperature drop marks the onshore movement of colder bottom water.

Repeated conductivity, temperature, and depth (CTD) sections along a line extending offshore across the shelf and upper slope at 39°N show this seasonal change in the temperature and density distribution over the shelf [*Huyer*, 1984]. In 1982 this section was occupied repeatedly before and after the spring transition [*Fleishbein et al.*, 1983*a*, *b*, *c*]. Selected sections (Figure 7) show that the midshelf temperature at 70 m fell by 1.0° to 1.5°C between March 1 and April 24, while the density anomaly σ_t increased from 26.0 to 26.5 mg cm^{-3}; the 70-m density difference across the shelf was approximately 0.9 mg cm^{-3} on April 24, in comparison to approximately 0.2 mg cm^{-3} on March 1. A month later, on May 26 and 27, bottom water over the shelf still had about the same density ($\sigma_t \approx$ 26.5) while shallower waters over the midshelf had increased in density (Figure 7), presumably because continued upwelling had advected the lighter waters offshore well beyond the upper slope. The region of greatest horizontal density gradient had also moved farther offshore, leaving a cross-shelf density difference of only 0.2–0.4 mg cm^{-3}; the midshelf region had lost most of its horizontal and vertical density gradients.

Figures 6 and 7 confirm that the transition event draws water that is 1°–2°C colder up onto the shelf all along the coast to a much greater extent than any of the previous southward wind events and that this cooler water remains over the shelf, at least through June. The cross-shelf density difference at 39°N (Figure 7) immediately after the transition is the same order of magnitude (1.0 mg cm^{-3}) as that reported by *Huyer et al.* [1979] at 45°N in 1975. In 1981 after the transition, bottom temperatures also stayed 1°–2°C lower than the annual mean until late summer, while alongshore currents alternated between northward and southward [SAHSB,

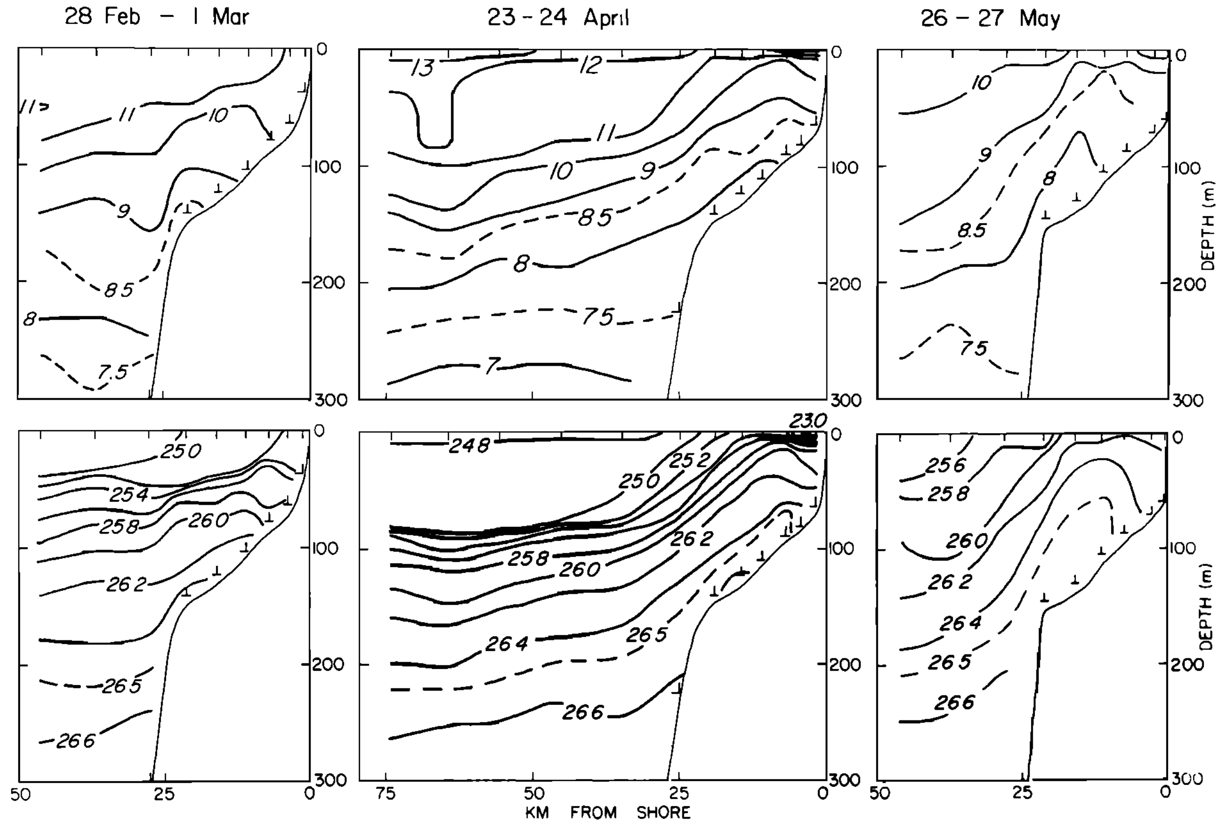

Fig. 7. Cross-shelf vertical sections of (top) temperature and (bottom) σ_t at 39°N for (left) February 28 to March 1, (middle) April 23 and 24, and (right) May 26 and 27, 1982. Contour intervals are in degrees Celsius and milligrams per cubic centimeter [from *Fleischbein et al.*, 1983*a*, *b*, *c*]. Station locations are indicated by the tick marks at the top of each figure and the perpendicular signs over the shelf.

Figure 12]. Thus the current and temperature data from the 2 years present a consistent picture of bottom temperatures that stay low while alongshore velocities fluctuate.

Time Histories of the 1982 Event at Individual Locations

Figure 8 presents time histories of the wind stress, sea level, alongshore currents, and temperatures from the shelf break and midshelf at 39°N for February through June 1982. The mooring and instrument depths presented here are similar to those at other latitudes shown below and allow a comparison of the north-south structure of the 1982 transition. *Lentz* [this issue] gives a more detailed account of the transition at the 39°N location.

At 39°N the wind event at the time of the transition (April 15–20) is quite similar to the earlier event around February 20–25, as are the currents generated over the midshelf. The drop in sea level and water temperatures are slightly greater following the April transition than after the earlier February event and may reflect the larger alongshore scale of the southward winds during the transition. In Figure 5 it can be seen that the -1 and -2 dyn cm^{-2} contours extend over approximately 1400 and 500 km during the transition, in comparison to 800 and 200 km, respectively, during the February 20 event. Strong northward winds after the February event reverse the upwelling process and return conditions to the winter regime.

At both midshelf and shelf break moorings the lowest instrument is approximately 20 m above the bottom, and both show the rapid drop to below 8°C during the transition (April 15–20) in Figure 8, also seen in the April 24 section in Figure 7. At a given depth the decrease in temperature is greater at midshelf than over the shelf break, and cross-shelf temperature differences of the order of 1°C develop at 35 m and 70 m. Vertical shear in the alongshore current over the shelf break lasts at least until May 25, but there is only a brief period of vertical shear over the midshelf before the currents reverse immediately after the maximum southward wind stress on April 18. Figure 7 shows the region of maximum cross-shelf density difference to have moved offshore past the midshelf by April 24, although it is still strong enough at the shelf break to maintain the vertical shear seen there in Figure 8. The 35-m and 70-m currents at the shelf break do not reverse and become northward during the wind relaxation of April 20–30, as they do over midshelf where the vertical shear is absent.

During much of the April 20 to May 20 period the cross-shelf temperature difference is greater at 25 m than at 70 m, and the vertical shear at the shelf break appears more constant between the 35-m and 70-m currents than between 70 and 110 m. This is reflected in the April 24 density section (Figure 7), which shows the main cross-shelf density difference to be concentrated above 70 m. The vertical shear and the cross-shelf temperature difference drop to zero during a period of low wind stress and northward barotropic currents in early May, then return and last until the end of May. Subsequently, the horizontal temperature difference and the vertical shear become intermittent, and the entire shelf experiences surface current reversals [*Beardsley and Alessi*, 1985].

Figure 9 shows data from the midshelf mooring at 41°N,

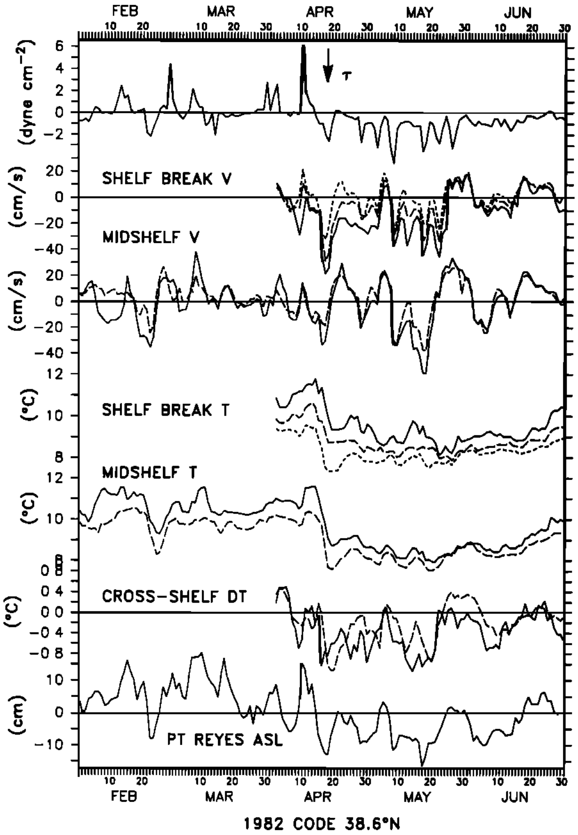

Fig. 8. Data from the moorings at 38.6°N (CODE) and nearby alongshore wind stress and sea level for February–June 1982. From top to bottom: alongshore calculated wind stress; alongshore currents from the shelf break mooring; alongshore currents from the midshelf mooring; temperatures from the shelf break mooring; temperatures from the midshelf mooring; cross-shelf temperature differences (midshelf-shelf break); and adjusted sea level from Point Reyes (38°N). Mooring data come from 35 m (solid line), 70 m (long-dashed line), and 110 m (short-dashed line).

approximately 220 km north of the 39°N mooring. The 41°N mooring, although at the same isobath as the midshelf mooring at 39°N, is farther from shore (14 km compared to 8 km) and closer to the local shelf break than the local midshelf. The wind forcing here is very similar to that at 39°N. Low sea levels persist for the first 2 months after the transition on April 15–20. The difference between the strong sea level response to this transition event compared to the weak response to the February 20–25 event is more pronounced at 41°N than at 39°N. Vertical shear in the alongshore current persists for at least a month after the transition, and the currents resemble those from the shelf break at 39°N. The vertical shear diminishes gradually and becomes negligible by late May, when currents are nearly barotropic with northward fluctuations. The period of vertical shear from April 18 to May 28 is characterized by initial rapid cooling at 70 m (as is seen at 39°N) and more gradual cooling at 35 m.

Data from 43°N (260 km to the north of the 41°N mooring) are shown in Figure 10; the midshelf and shelf break moorings there are 11 km and 17 km from shore, about 3 km farther offshore than those at 39°N. Local wind forcing of the transition event appears to be weaker than farther south, but the sea level response is greater. Local southward winds during the February 20–25 wind event are very weak, but there is a drop in the temperature at the deepest instrument over the shelf

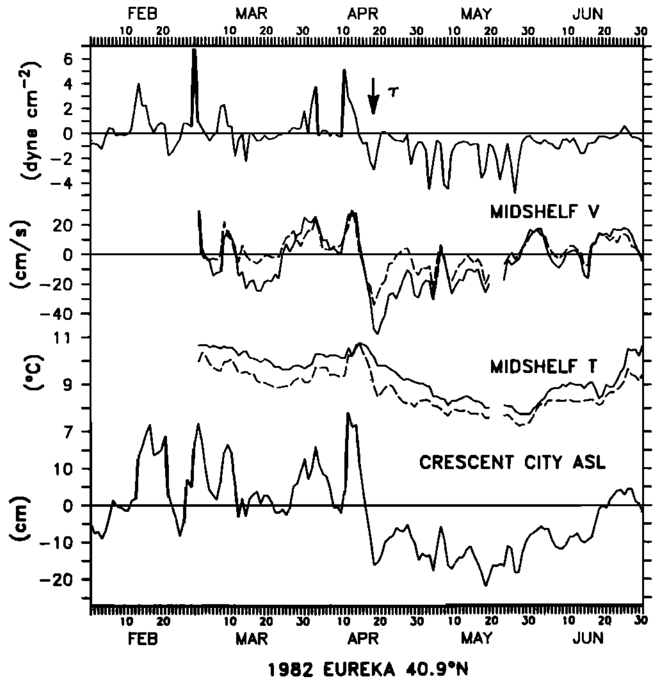

Fig. 9. Data from the midshelf mooring at 40.9°N in 1982. Notation is the same as is in Figure 8.

break and southward currents are observed over both the midshelf and shelf break; these may be responses to the stronger forcing farther south, indicated in Figure 5. The data from the shelf break are complete until May 19 and show that the vertical shear after the April 18 transition appears first in the lower water column (between 70 m and 110 m) and later

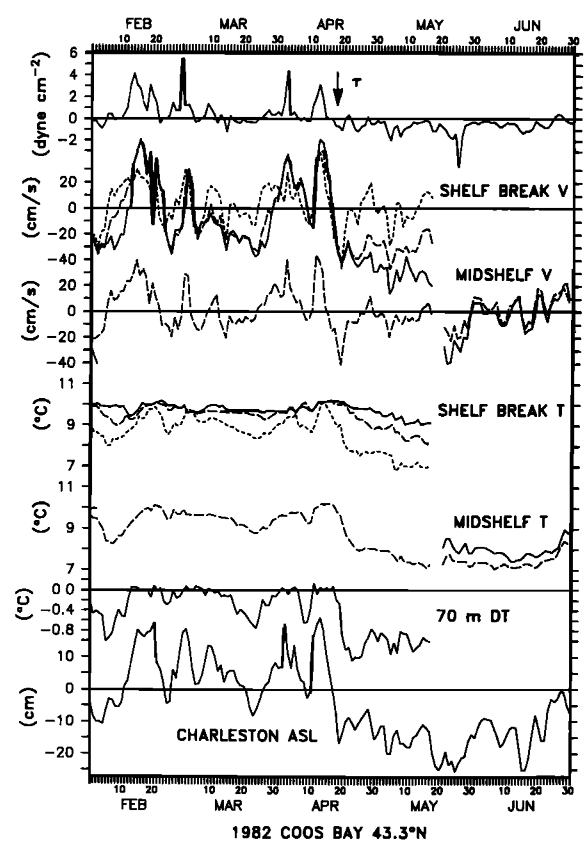

Fig. 10. Data from the midshelf and shelf break moorings at 43.3°N in 1982. Notation is the same as is in Figure 8.

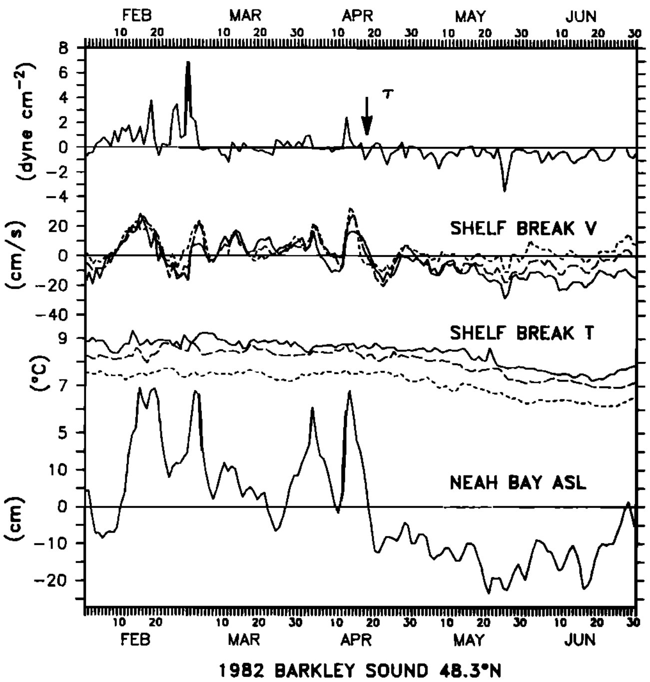

Fig. 11. Data from the shelf break mooring at 48.3°N in 1982. Meter depths for this mooring are 50 m (solid), 100 m (long-dashed line), and 150 m (short-dashed line) in 210 m of water. Other notation is the same as is in Figure 8.

at middepth (between 35 m and 70 m). No decrease of vertical shear or of cross-shelf temperature difference at 70 m occurs by the end of the shelf break record on May 19. The vertical shear at 43°N developed more slowly than at 39°N, and once established, the vertical shear and cross-shelf temperature difference were more persistent at 43°N than at 39°N. The current reversal at 35 m and 70 m seen at 39°N in early May is not seen at 43°N. After May 19 the midshelf records show a gradual decrease in the vertical shear in late May and early June as the 35-m temperature drops to within 0.5°C of the 70-m temperature. Unlike the midshelf currents farther south, this weak vertical shear persists until the end of June. A CTD section off 43°N on May 20 [*Fleischbein et al.*, 1983*c*] shows a region of strong cross-shelf density gradient over the shelf break, unlike the diffuse gradients found farther offshore on May 26 and 27 at 39°N (Figure 7). The offshore water at 43°N is much fresher and lighter than at 39°N, suggesting the importance of the Columbia River plume in maintaining the cross-shelf density gradient at 43°N.

At the 48°N mooring (580 km north of 43°N), data from the shelf break show that the summer regime in currents and temperatures takes longer to become established, but conditions then remain much more constant (Figure 11). The shelf near this mooring is much wider than at any of the other mooring locations, and the mooring is 75 km from shore [SAHSB, Figure 1]. As is noted above, measurements from midshelf at this latitude during previous summers showed northward monthly mean midshelf currents [*Freeland et al.*, 1984], similar to the monthly mean currents in summer at 43°N and 39°N seen in 1982. Midshelf currents at 48°N were not availble during 1982 for comparison to the other currents presented here. Wind stresses at 48°N are similar to those at 43°N, and the sea level response between April 15 and 20 is rapid, leading to persistently low levels. The equatorward velocities at the time of the transition are not as strong as farther south, and an immediate signal is not seen in even the lowest temperatures (150 m in water 210 m deep), possibly because of the time required to draw water up over the large shelf and be mixed upward and outward to the 150-m shelf break location. Temperatures drop very gradually, beginning first at 150 m in late April. Persistent vertical shear develops first between the lower (150 m and 100 m) alongshore currents in early May and later between the upper (100 m and 50 m) currents in the second half of May; this vertical shear is very steady.

Current and temperature measurements from the mooring at 37°N, which are not shown, come only from the 70-m depth on the midshelf mooring and are very similar to the 70-m midshelf data at 39°N. The picture in the south at 35°N in 1982 (Figure 12) is different from that between 37°N and 48°N. Winds in February through mid-April are alternating but southward in the mean, becoming more strongly southward at the time of the northern April 15–20 transition. During most of April there is persistent southward flow over both the midshelf and shelf break, persistent shear at the shelf break, and a persistent cross-shelf temperature gradient. However, this period of sheared southward flow begins 10–15 days earlier than in the north, its onset does not coincide with a drop in sea level (which is aleady below the annual mean by April), and the cross-shelf temperature difference is caused by a rise in the upper shelf break temperatures, rather than a drop in the lower midshelf temperatures. Warm water appears to move onshore with a southward velocity component before the stronger southward winds of the mid-April spring transition and disappears afterward, leaving alternating northward and southward currents during the stronger southward winds of May and June. At midshelf there is a gradual cooling by

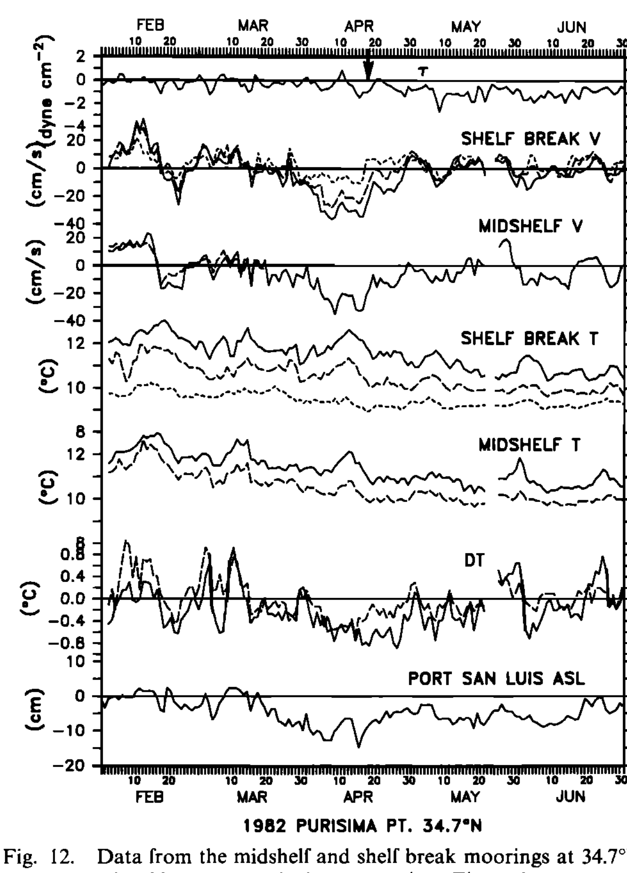

Fig. 12. Data from the midshelf and shelf break moorings at 34.7°N in 1982. Notation is the same as is in Figure 8.

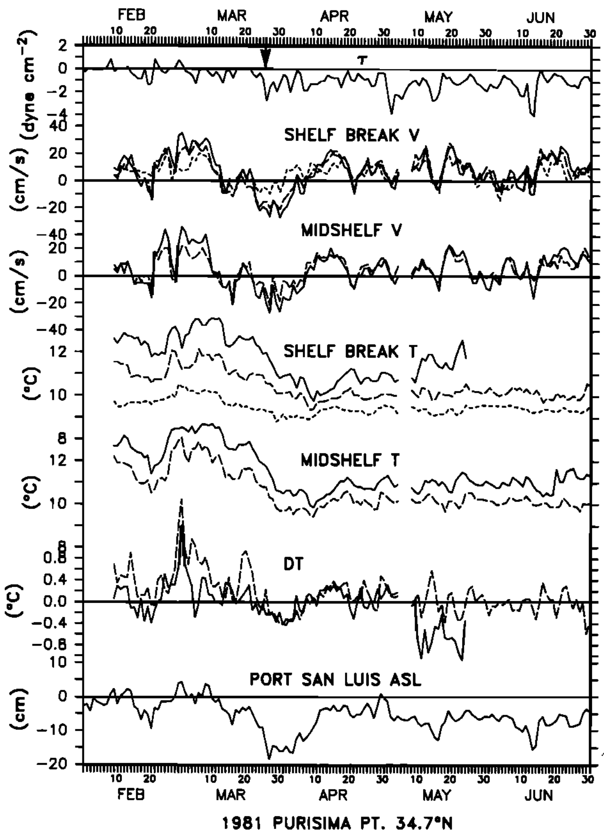

Fig. 13. Data from the midshelf and shelf break moorings at 34.7°N in 1981, similar to Figure 12.

1°–1.5°C over the 5-month period, interrupted by the warming associated with the southward currents in April.

Data from the same location in 1981 (Figure 13) show a more normal coastal upwelling picture, at least for a brief period around the late March spring transition. When winds become strongly southward about March 25, currents at the shelf break become southward with a vertical shear between 70 m and 110 m, and sea levels and temperatures drop, with more rapid cooling at midshelf and a slight cross-shelf temperature gradient. This lasts only until April 10, when currents resume alternating about a northward mean in opposition to stronger southward winds, while temperatures and sea level rise but do not return to their pretransition values. Thus in 1981 the behavior at 35°N could be said to be a briefer version of that seen at 39°N in 1982: rapid onset and then decay of a cross-shelf temperature gradient and vertical shear of the southward alongshore currents after the transition, returning to alternating currents after the shelf break temperatures have cooled to approximately the same values as those at midshelf.

Data from moorings at 42°N and 48°N are also available at the time of the 1981 transition and are compared to the 35°N data in Figure 14. The southward currents increase and sea level and bottom temperatures drop at 35°N in apparent response to southward wind stress between March 21 and 24, while northward winds at 42°N and 48°N (Figure 3) continue to force northward currents and high sea levels and temperatures there. Large-scale southward winds on March 26–28 (Figure 3) force strong southward currents and lower sea levels at both 35°N and 42°N (separated by 830 km) and soon after at 48°N (another 740 km to the north). Posttransition current and temperature data from these moorings and others at 39°N and 43°N [*Winant and Bratkovich*, 1983; *Brown et al.*, 1983; *Denbo et al.*, 1984] indicate that the cross-shelf temperature difference and vertical shear at the shelf break lasted longer than in 1982 (until the end of June or longer) and were again stronger and more lasting at 43°N than at 39°N. It appears that the 1981 spring transition was of a larger scale (1500 km, extending to 35°N), as is noted above from the sea level and wind data in Figure 3, and that the early summer regime was more persistent in southward currents and in vertical shear over the shelf break than in 1982. In both years the response was slower and more persistent in the north.

DISCUSSION

To extend the discussion beyond the 1981 and 1982 periods, alongshore wind stress and sea level data for 9 years (1971–1975 and 1980–1983) have been used to form a "composite" month of data, showing the average sequence of events from 15 days before to 15 days after the spring transition. The date of each year's transition was based on sea level data from 41.8°N; that date was designated day 16 of a 30-day period, and the 30-day records for all 9 years at each location were ensemble-averaged to form composite time series, centered on the transition. Contours of these wind stress and sea level time series are presented in Figure 15. Contours of the 7 individual years not previously shown are presented in Figure 16.

Alongshore Scale of the Spring Transition

On the basis of the drop from the 0- to the −5-cm contour of the composite sea level data in Figure 15 as an indication of

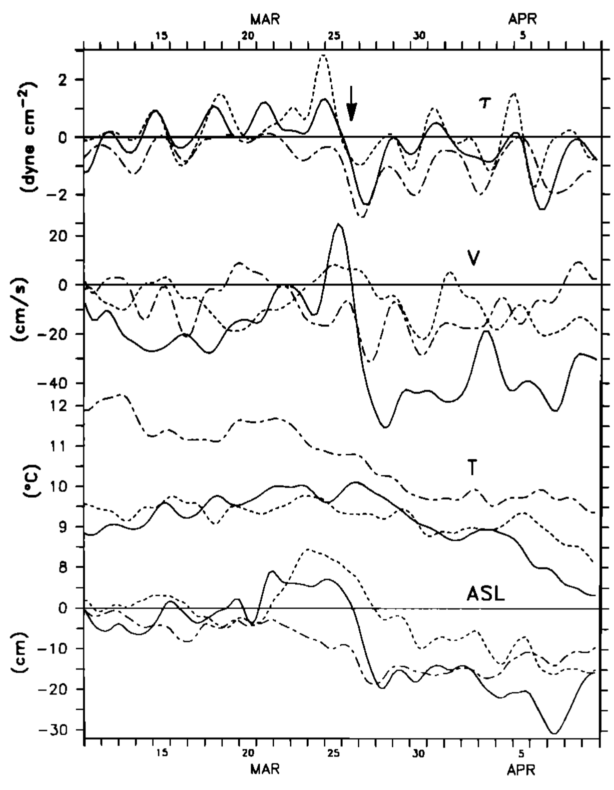

Fig. 14. Comparison of alongshore wind stress (top), alongshore velocity at 35–50 m depth (second from top), water temperature from the bottom instrument (third from top), and sea level (bottom) for March 11 to April 9, 1981. The moorings come from the shelf break at 48°N (short-dashed line), midshelf at 42°N (solid line), and midshelf at 35°N (long- and short-dashed line).

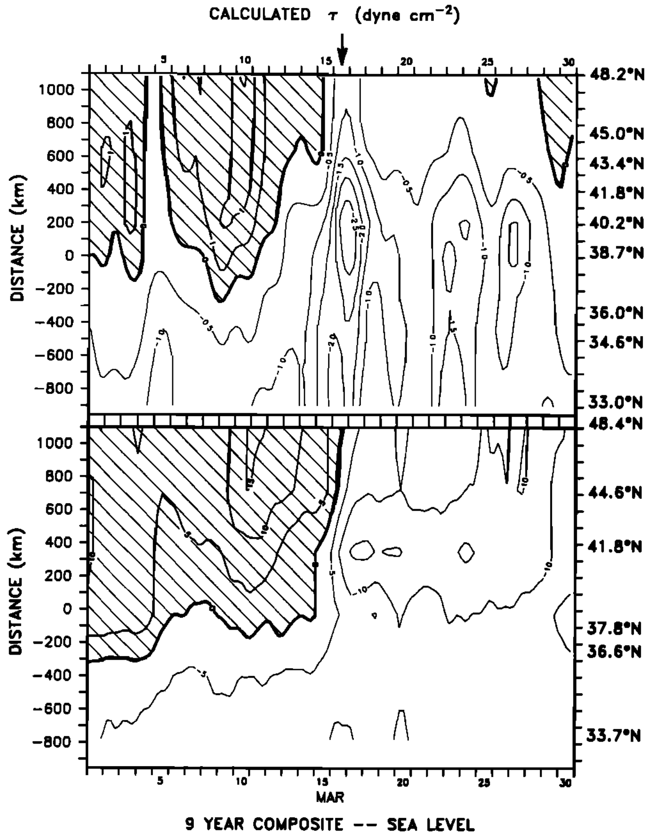

Fig. 15. Contours of the composite average time series of alongshore calculated wind stress and adjusted sea level, formed from 9 years of data (1971–1975 and 1980–1983), centered on a date chosen for each years's transition event at 41.8°N, which appears here as March 16 (not the real date). Areas of positive values are indicated by hatching. Contour intervals are 0.5 dyn cm^{-2} and 5 cm. Station locations are indicated on the right by their latitudes.

the spring transition, the alongshore scale of the response is of the order of 1200 km or more. The strongest response, indicated by the −10-cm contours, has a smaller scale of roughly 800 km. The alongshore scale of the wind stress associated with the transition is larger than the sea level response defined above: 1800 km for the −1 dyn cm^{-2} contour and 1500 km to 1300 km for the −1.5 and −2 dyn cm^{-2} contours. Using the 9 individual years seen in Figures 3, 5, and 16, the scales of the −1 dyn cm^{-2} and −2 dyn cm^{-2} contours have ranges of 1500–2000 km and 500–2000 km, respectively; the scales of the −10-cm and −15-cm sea level contours have ranges of 200–2000 km and 0–1500 km, respectively. The 1981 and 1982 data (Figures 3 and 5) indicate that the alongshore scale of the strong southward winds (−2 dyn cm^{-2}) was 1300 km in 1981 and 500 km in 1982, while the scale of the rapid drop in sea level to 15 cm below the annual mean was 1100 km in 1981 and 400 km in 1982. Thus differences between 1981 (stronger, larger-scale forcing and response) and 1982 (weak, smaller-scale forcing and response) represent the normal variability seen in the 9 years of data, though not the extremes of variability seen by comparing the weak forcing and response in 1974 to the extreme forcing and response of 1975. The current and temperature data for these 2 years also have alongshore scales in the 1000–1500 km range, indicated by the response from 35°N to 48°N (over 1500 km) in 1981 (Figure 14) and 39°N to 48°N (about 1000 km) in 1982 (Figure 6).

Since the winds used in this analysis were calculated from smoothed pressure fields on a 3° grid, they cannot represent small alongshore scales, and it is natural to ask if measured winds from coastal locations show the same alongshore structure. Examination of measured winds from 1981–1983 [e.g., SAHSB, Figure 4*b*; *Halliwell and Allen*, 1985] show that the wind events associated with the spring transition in those years had alongshore scales of the order of 1000 km in 1981 and 1982 and 1300 km in 1983 and were similar in structure to the corresponding events in the pressure-derived winds.

Sequence of Events and Persistence of the Features

The composite picture of wind stress and sea level in Figure 15 shows the typical sequence of events seen in the individual years. Monthly mean wind stress is climatologically southward all year south of 35°–37°N [SAHSB] and becomes more strongly southward some time before the main transition, while wind stress in the north alternates between brief periods of southward wind stress (usually less than 2 dyn cm^{-2}) and longer periods of stronger northward wind stress. Sea levels drop slowly in the south and are forced down briefly in the north by the southward events, only to be forced up again by the northward events. The large-scale transition north of 37°N occurs as the region of southward wind stress moves progressively north over a 3- to 10-day period, usually including a final northward event in the north. Following the northward movement of the southward winds, a several-day period of large-scale southward wind stress of 2 dyn cm^{-2} or more produces the large-scale response in sea level. Wind fields for the 1981 (Figure 4) and 1982 events have the same character, showing northward (cyclonic) winds in the north and southward (anticyclonic) winds in the south and the northward movement of the southward winds over the large-scale coastal domain.

The composite of 9 years of alongshore wind stresses shown in Figure 15 indicates that a major change occurs in the coastal alongshore winds and that this is followed rapidly by a large-scale drop of coastal sea levels. This pattern of winds is consistent with the strengthening and northward spread of the North Pacific high, following passage of a late winter storm through the northern part of the domain. A detailed description of the cause of this large-scale atmospheric transition is not readily available in the literature. *Lahey et al.* [1958] present 5-day mean sea level pressure maps from throughout the year, formed by compositing 20 years of historical data according to calendar dates. These show the weakening, splitting, and northward displacment of the Aleutian low-pressure center (from approximately 50°N to 55°N) and the northward movement of the North Pacific high-pressure system in early April, in agreement with the range of dates for the spring transition determined here from 9 years of sea level data at 41.8°N (March 22 to April 18). *Lentz* [this issue] also describes the movement of these pressure systems (his Figure 21), on the basis of *Bryson and Lahey*'s [1958] analysis of the 5-day mean sea level pressure maps shown by *Lahey et al.* [1958]. The 5-day mean climatological pressure maps also show the growth of a low-pressure region over Mexico in February that moves into the southwest United States during March, causing the increase in southward winds over the coast off Baja California that may be linked to the gradual drop in sea level off southern California. A clearer description of the atmospheric transition might be formed by compositing

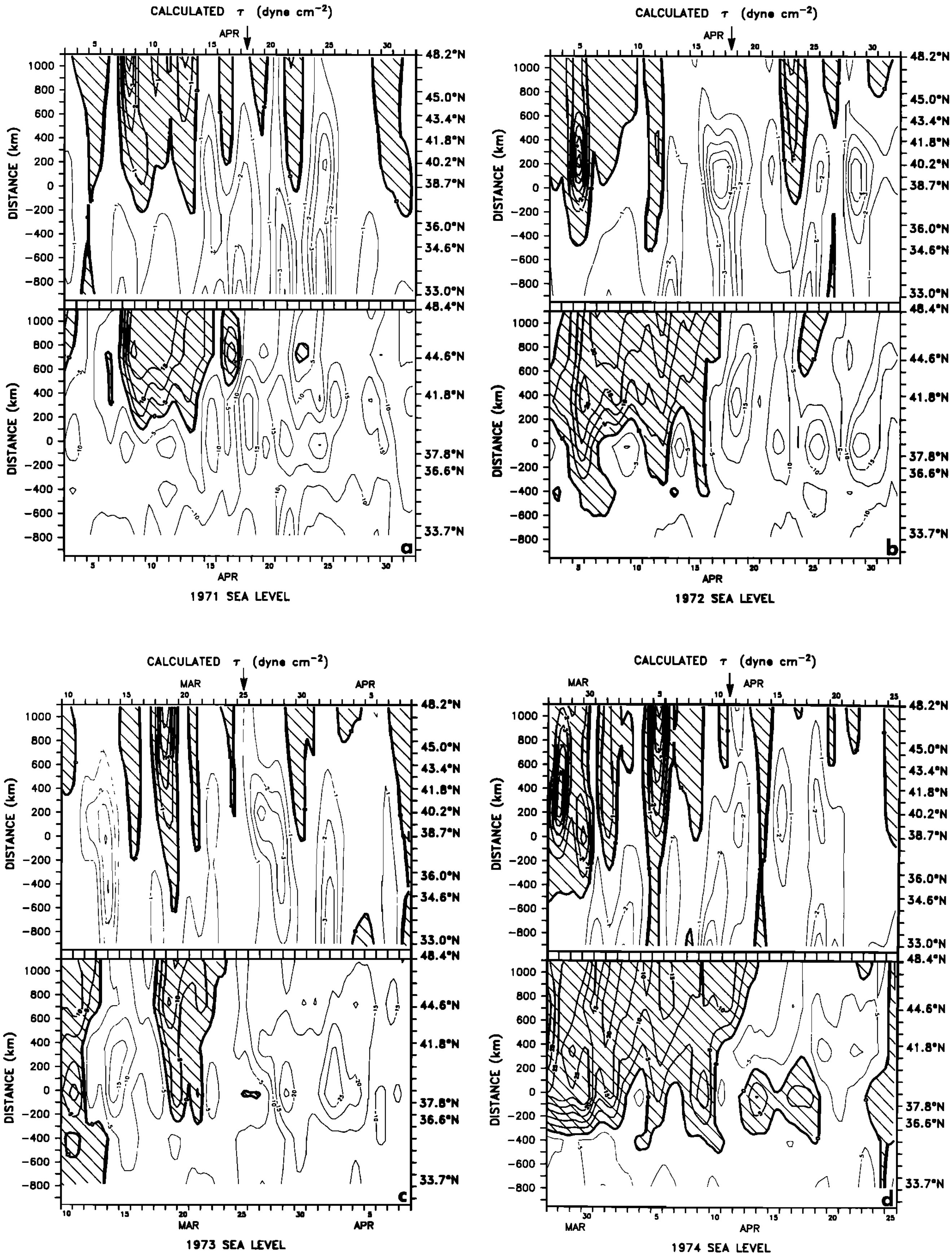

Fig. 16. Contours of the historical alongshore calculated wind stress and adjusted sea level for 7 years (1971–1975, 1980, and 1983). Contour intervals are 1.0 dyn cm^{-2} and 5 cm.

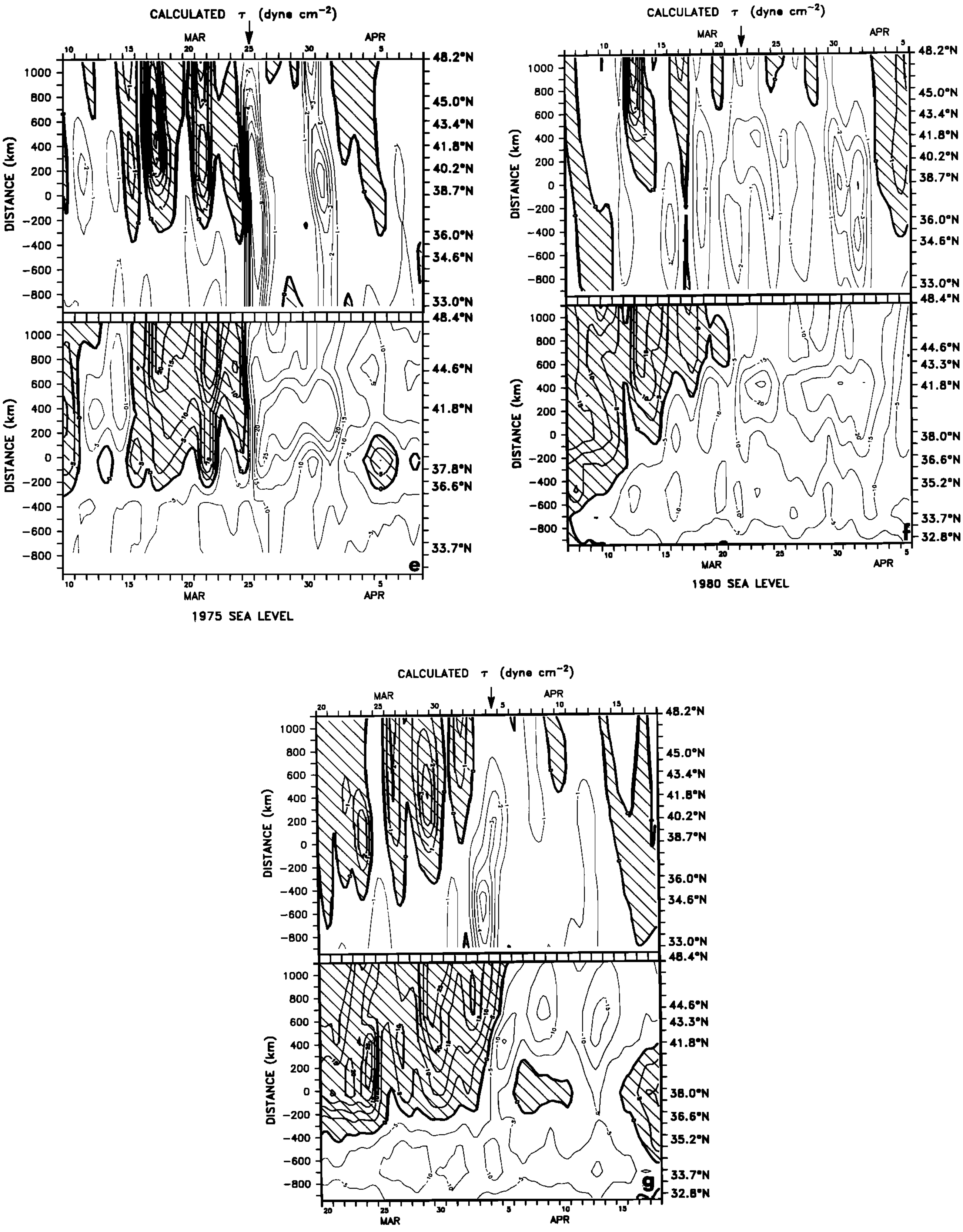

Fig. 16. (continued)

the large-scale fields of historical atmospheric variables around the time of the oceanic transition (using sea level to indicate the timing of the oceanic transition) as is done in forming Figure 15. This would avoid the smearing of features related to the event caused by averages based on calendar dates, since the date of the event varies from year to year.

The current and water temperature data indicate that southward currents, vertical shear of those currents over the shelf break, upwelling of cold water, and a cross-shelf temperature gradient persist for at least a few weeks following the transition in sea level. This is qualitatively similar to the sequence of events seen at 45°N in 1973 and 1975 [*Huyer et al.*, 1979]. The amount of time it takes to set up the baroclinic summer regime over the shelf break and the length of time it persists there seem to increase progressively from 39°N (or from 35°N in 1981) to 48°N. These time differences may be due to differences in the shelf width and/or the strength of the local wind. At 39°N the cross-shelf temperature gradient and vertical shear over the shelf break only persist for the first month after the transition or less and are variable even during this period. CTD data from 39°N in 1982 (Figure 7) show that a cross-shelf density difference of the order of 1.0 mg cm^{-3} seen immediately after the transition in late April is reduced to values of the order of 0.2 mg cm^{-3} by the end of May, similar to values observed before the transition. The May CTD section shows the density front to have moved offshore of the shelf break and weakened. In 1981 at 39°N, cross-shelf density differences of 0.6 mg cm^{-3} in mid-April (after the late March transition) are reduced to approximately 0.2 mg cm^{-3} or less by late April, when the density front is again found farther offshore [*Huyer*, 1984]. With the loss of the mean horizontal density gradient and vertical shear, the barotropic fluctuations in the alongshore current result in surface current reversals over the shelf. At locations farther north the cross-shelf density gradient and mean vertical shear take progressively longer to develop at the shelf break, as is indicated by the current and temperature data from 39°N and 43°N presented in Figures 8 and 10; once established, the density front appears to be maintained longer over the shelf break.

At the southern end of the domain (35°N), the current and temperature behaviors in 1982 are quite different from those in the domain north of 37°N. During the larger-scale transition in 1981 this region does appear to be included in the northern regime for a very brief period lasting less than a month. The sea level data shown in Figures 3, 5, 15, and 16 indicate that only in a few years does the sea level south of 37°N show a sharp drop at the same time as the northern sites, though there are often strong southward winds in the south. The lack of correspondence between local wind stress forcing and sea level and current response around 35°N has been noted by other authors [*Brink et al.*, 1984; *Brink and Muench*, 1986; *Denbo and Allen*, this issue], but the dynamics responsible for this behavior have not been determined.

Using simple models of sustained coastal upwelling in the presence of wind-generated mixing and surface heating, *de Szoeke and Richman* [1981, 1984] have shown that the upwelling front can be advected several Rossby radii offshore, leaving a region of low-density gradients between the coast and the front. This is the simplest explanation for the observations off northern California, where strong southward winds are often sustained for more than a week and the shelf is usually narrower than 25 km. The presence of the upwelling front offshore of the shelf break is suppoted by data from an upper slope mooring over the 500-m isobath at 39°N in 1982 [*Winant et al.*, 1985]. At that location, vertical shear between the 70-m and 150-m alongshore currents developed at the time of the transition and lasted until at least the end of June, more than a month longer than the shear at the shelf break. In the extreme north (48°N) the shelf is 75 km wide, and the weaker alternating Ekman transport makes it easier to maintain the density gradient and vertical shear over the shelf through the summer. An additional factor off central Oregon is the presence of lighter Columbia River water offshore in the spring and summer; its influence is strongest in the region between 42°N and 46°N [*Huyer*, 1983]. This lighter water, along with the alternating winds found in the north, may help keep the density front closer to the coast off Oregon than farther south.

Characteristics of the Large-Scale Wind Forcing and Response

The composite picture of wind stress and sea level in Figure 15 indicates that the spring transition wind event is generally of large alongshore scale. The historical data show, however, that subregions of the domain between 33°N and 48°N (approximately 2000 km) can be forced separately. In 1971 (Figure 2), winds became southward and sea levels lowered south of 38°N in February (the earliest date observed), while they continued to alternate north of 38°N until April, dividing the coast into two large-scale regions of 500 to 1000 km. In 1980 (Figure 16*f*) the sea level transition occurred at progressively northward locations as a response to a sequence of three or four 1- to 2-day events with alongshore scales of 800 km and larger, over a 12-day period. The transition in sea level thus appears to be able to respond to persistent wind forcing in regions of 500 km and larger.

Temperature data from 1982 (Figure 6) provide evidence that large-scale wind forcing is more effective in drawing up the denser water and setting up the spring-summer regime than smaller-scale events of similar magnitude. Southward wind events of 1 dyn cm^{-2} result in temperature drops of 0.5° to 1.0°C around February 5 and 20–25. The alongshore scales of these wind events were of the order of 400 km and 800 km, respectively. These temperatures increased again when the southward winds relaxed but before strong northward winds appeared, showing their transient nature. This can also be seen in Figure 8, where the transient February 20–25 and final April 15–20 events can be compared at 39°N. The final transition involves much larger scale forcing and results in a more rapid and permanent response in water temperature.

Several features of the large-scale spring transition suggest that it should be considered a nonlocal event, with characteristics consistent with coastal trapped wave theory. In Figure 15 the maximum response in sea level occurs several hundred kilometers north of the maximum in the southward wind stress. This is similar to the characteristics of sea level response to smaller-scale wind stress events and is consistent with results from coastal trapped wave theory [*Halliwell and Allen*, 1981]. These small-scale southward wind stress events cause upwelling and raise the local isopycnals over the shelf, but the small-scale density anomaly created by the local upwelling can (according to shelf wave theory) propagate away poleward and alongshore when the wind relaxes. Such an event is suggested in Figure 10 by the drop in bottom temperature (and increase in southward velocities) over the shelf break at 43°N in late February, apparently in response to the small-scale southward wind event centered farther south around 39°N (Figures 5 and 8). In contrast, a lage-scale (1500–2000 km) southward wind event causes local upwelling and isopycnal displacements over a large domain. Northward propagation then maintains the upwelling regime in the northern region of the wind forcing. If the wind also propagates to the north, the response to the local wind may combine with the northward propagating response to the winds farther south to drive an even more efficient upwelling process. With the relaxation of the winds the water is more uniformly cold and dense over a large region along the coast, and the predominantly alongshore currents and wave propagation will not as easily alter the characteristics of the shelf water. Thus large-scale southward wind events propagating northward theoretically provide the most efficient mechanism for drawing denser water over the shelf and should result in a more persistent local upwelling regime than would winds of similar magnitude with smaller alongshore scales.

K. H. Brink (personal communication, 1986) has pointed out that other characteristics of the spring transition seen in this data are also consistent with continental shelf wave dynamics. If the spring transition is thought of as a response involving a combination of the first several coastal trapped wave modes, it can be shown that the signal in pressure (sea level) will be dominated by the lowest mode. The higher modes will contribute somewhat more to the alongshore velocity signal and proportionately even more to the density (temperature) signal. The higher modes travel more slowly and tend to smear the signal over a greater distance and, consequently, over a longer period of time at a given location along the coast. This is consistent with the longer time required to see the spring and summer regimes in the temperature (Figure 6) north of the region of strongest wind forcing, in comparison to the rapid response in sea level.

Though large-scale northward propagating wind systems are theoretically more efficient in forcing strong upwelling, the observations show that they are not necessary for the creation of a strong transition. Examples of the transition beginning in the north and extending to the south can be seen in the historical data. In 1973 (Figure 16*c*), strong southward winds begin on March 25 in the north and extend to the south over the next 2 days, and the drop of sea level to 10 and 15 cm below the mean also progresses to the south. In 1975 (Figure 16*e*) the transition on March 24–26 involves the strongest wind forcing seen in the spring transition events, with southward wind stresses of 4–6 dyn cm^{-2} beginning slightly earlier in the north. Sea levels also drop slightly earlier in the north in this year, as is pointed out by *Huyer et al.* [1979]. Examples can also be found, however, of wind events progressing from north to south and sea level responding from south to north, as is seen April 15–20, 1972, and April 28–30, 1972 (Figure 16*d*). During many of the events in various years the drop to the lowest sea levels appears to progress from south to north, even if the initial drop to 5–10 cm below the mean progresses from north to south (for example, on March 26, 1975, and March 14, 1973). Thus the coastal ocean's preference for poleward propagation can often be seen in the sea level data, even when absent in the wind stress.

CONCLUSIONS

1. The spring transition in coastal sea level, currents, and temperatures is a large-scale phenomenon, driven by the large-scale wind system. The alongshore scale of the southward wind forcing of magnitude 2 dyn cm^{-2} is typically of the order of 1500 km, as is seen in the 9-year composite (Figure 15), with strongest winds between 38°N and 42°N; the scale of the forcing ranges from 500 to 2000 km in the individual years (Figures 3, 5, and 16). The alongshore scale of the rapid sea level drop to 10 cm below the annual mean is typically of the order of 800 km, as is seen in the composite, centered around 42°N; the scale ranges from 200 to 2000 km in individual years, with the scale of the sea level response varying in the same sense as the scale of the wind stress forcing. South of 37°N, the response to the wind event is weak, if present at all.

2. The initial sequence of events is similar at the locations sampled north of 37°N, following the pattern seen at 45°N in 1973 and 1975 [*Huyer et al.*, 1979]. Southward winds over a several-day period force low sea levels and upwelling of denser water along the shelf, which results in a horizontal density gradient across the shelf and a mean vertical shear in the alongshore (southward) current. The difference between locations is that this regime is less persistent over the shelf and shelf break in the region from 38°N to 42°N, where the wind stress is greatest and the shelf is narrow. At these latitudes the upwelling front is moved offshore past the shelf break in the first 1 to 2 months, leaving a more homogeneous water mass over the shelf, with little mean vertical shear. Barotropic fluctuations then allow northward surface currents over the entire shelf area. North of 42°N, the weaker wind stress alternates between southward and northward, the horizontal density gradient and vertical shear persist over the wider shelf and shelf break for longer periods (3–6 months), and surface currents remain predominantly southward. Fresh water from the Columbia River plume may help to maintain the upwelling front closer to the coast north of 42°N. South of 37°N, the southward wind stress becomes stronger, and sea levels begin lowering during the month preceding the stronger transition wind event. A rapid lowering of sea level there occurs at the same time as the northern transition event only in a few years. The current and temperature data from 35°N show the transition event in 1981 but not in 1982; the period of southward flow and low sea levels lasts for less than a month in 1981, though winds remain southward.

3. The behavior of the surface winds during the transition is related to changes in the large-scale atmospheric sea level pressure systems. The appearance of a low-pressure system over Mexico and its movement into the southwest in February and March, while high pressure builds over the ocean at the same latitude to the west, may result in the southward winds and lower sea levels south of 37°N before the northern transition. The weakening and northward displacement of the Aleutian low from approximately 50°N to 55°N in late March or early April accompanies a strengthening and northward movement of the North Pacific high. The transition event often occurs when a late winter storm passes through the middle of the 33°N to 48°N domain and creates an episode of strong northward winds there, followed by a spreading of the high-pressure region and southward winds along the coast as the storm moves eastward. The strongest transitions may occur when this storm remains over the western continental United States for several days, subjecting the coastal region to strong pressure gradients and southward winds, as occurred in 1981.

4. The ability for disturbances to propagate poleward as coastal trapped waves appears to give a nonlocal nature to the

large-scale spring transition. Evidence for this is provided by the general occurrence of the maximum response of sea level at an alongshore location several hundred kilometers north of the maximum in wind stress forcing and by the general northward progression of the sea level fluctuations involved in the adjustment over several days following the initial response. In 1982 the alongshore velocity and the temperature signal also progress northward, and temperature progresses more slowly than velocity. The slower response of temperature is also consistent with results from models of coastal trapped waves (K. H. Brink, personal communication, 1986).

5. It is not necessary for the wind event to progress northward, and examples of southward progression of forcing and response can be found in the historical wind and sea level data. The coastal ocean's preference for poleward propagation, however, can be seen in the sea level data, in examples of events which progress southward in wind stress and northward in sea level response. This again demonstrates the nonlocal nature of the transition.

Acknowledgments. This work was supported by NSF under grants OCE-8405232 and OCE-8026131. Conversations with S. Lentz and K. Brink were especially helpful during the writing of the paper. H. Freeland kindly supplied the Canadian data, and R. C. Beardsley supplied data from 39°N. D. Denbo, B. Halliwell, H. Pittock, P. Newberger, and C. Allessi helped process the current meter, wind, and sea level data. K. Daniels helped with the graphics.

REFERENCES

Allen, J. S., and D. W. Denbo, Statistical characteristics of the large-scale response of the coastal sea level to atmospheric forcing, *J. Phys. Oceanogr.*, *14*, 1079–1094, 1984.

Bakun, A., Coastal upwelling indices, west coast of North America, 1946–71, *Tech. Rep. NNFS SSRF-671*, 103 pp., Natl. Oceanogr. and Atmos. Admin., Seattle, Wash., 1973.

Beardsley, R. C., and C. A. Alessi, CODE-2: An array description of the surface wind and near-surface currents, in CODE-2: Moored Array and Large-Scale Data Report, *Tech. Rep. 85-35*, edited by R. Limeburner, pp. 109–132, Woods Hole Oceanogr. Inst., Woods Hole, Mass., 1985.

Blumberg, A. F., L. H. Kantha, J. H. Herring, and G. L. Mellor, California shelf physical oceanography circulation model, appendix C.1, Atmospheric forcing, *Rep. 88 C.1*, 171 pp., Dynalysis of Princeton, Princeton, N. J., 1984.

Brink, K. H., and R. D. Muench, Circulation in the Point Conception–Santa Barbara channel region, *J. Geophys. Res.*, *91*, 877–895, 1986.

Brink, K. H., D. W. Stewart, and J. C. Van Leer, Observations of the coastal upwelling region near 34°30′N off California: Spring 1981, *J. Phys. Oceanogr.*, *14*, 378–391, 1984.

Brown, W. S., J. D. Irish, and A. W. Bratkovich, CODE-1: Moored temperature and conductivity observations, in CODE-1: Moored Array and Large-Scale Data Report, *Tech. Rep. 83-23*, edited by L. K. Rosenfeld, pp. 81–116, Woods Hole Oceanogr. Inst., Woods Hole, Mass., 1983.

Bryson, R. A., and J. F. Lahey, The march of seasons, *Rep. ASTIA AO-1525 00*, 41 pp., Dep. of Meteorol., Univ. of Wisconsin, Madison, 1958.

Denbo, D. W., and J. S. Allen, Large-scale response to atmospheric forcing of shelf currents and coastal sea level off the west coast of North America: May–July 1981 and 1982, *J. Geophys. Res.*, this issue.

Denbo, D. W., K. Polzin, J. S. Allen, A. Huyer, and R. L. Smith, Current meter observations over the continental shelf off Oregon and northern California, February 1981–January 1984, *Data Rep. 112*, Coll. of Oceanogr., Oregon State Univ., 1984.

de Szoeke, R. A., and J. G. Richman, The role of wind-generated mixing in coastal upwelling, *J. Phys. Oceanogr.*, *11*, 1534–1547, 1981.

de Szoeke, R. A., and J. G. Richman, On wind-driven mixed layers with strong horizontal gradients—A theory with application to coastal upwelling, *J. Phys. Oceanogr.*, *14*, 363–377, 1984.

Fleischbein, J., W. E. Gilbert, A. Huyer, and R. Schramm, Hydrographic data from the second Coastal Ocean Dynamics Experiment: R/V *WECOMA*, leg 0, 26 February–1 March 1982, *Data Rep. 101*, 54 pp., Sch. of Oceanogr., Oregon State Univ., 1983*a*.

Fleischbein, J., W. E. Gilbert, and A. Huyer, Hydrographic data from the second Coastal Ocean Dynamics Experiment: R/V *WECOMA*, leg 6, 18–24 April 1982, *Data Rep. 102*, Sch. of Oceanogr., Oregon State Univ., 1983*b*.

Fleischbein, J., W. E. Gilbert, and A. Huyer, CTD observations off Oregon and California: R/V *WECOMA* and Code 2, leg 8, 18 May–4 June 1982, *Data Rep. 104*, 149 pp., Sch. of Oceanogr., Oregon State Univ., 1983*c*.

Freeland, H. J., W. R. Crawford, and R. E. Thomson, Currents along the Pacific coast of Canada, *Atmos. Ocean*, *22*, 151–172, 1984.

Halliwell, G. R., Jr., and J. S. Allen, CODE-1: Large-scale wind and sea level observations, in CODE-1: Moored Array and Large-Scale Data Report, *Tech. Rep. 83-23*, edited by L. K. Rosenfeld, pp. 139–185, Woods Hole Oceanogr. Inst., Woods Hole, Mass., 1983.

Halliwell, G. R., Jr., and J. S. Allen, Large-scale sea level response to atmospheric forcing along the west coast of North America, summer 1973, *J. Phys. Oceanogr.*, *14*, 864–886, 1984.

Halliwell, G. R., Jr., and J. S. Allen, CODE-2: Large-scale wind and sea level observations, in CODE-2: Moored Array and Large-Scale Data Report, *Tech. Rep. 85-35*, edited by R. Limeburner, pp. 179–233, Woods Hole Oceanogr. Inst., Woods Hole, Mass., 1985.

Halliwell, G. R., Jr., and J. S. Allen, The large-scale coastal wind field along the west coast of North America, 1981–1982, *J. Geophys. Res.*, this issue.

Huyer, A., Coastal upwelling in the California current system, *Prog. Oceanogr.*, *12*, 259–284, 1983.

Huyer, A., Hydrographic observations along the CODE central line off northern California, 1981, *J. Phys. Oceanogr.*, *14*, 1647–1658, 1984.

Huyer, A., R. L. Smith, and E. J. Sobey, Seasonal differences in low-frequency current fluctuations over the Oregon continental shelf, *J. Geophys. Res.*, *83*, 5077–5089, 1978.

Huyer, A., E. J. Sobey, and R. L. Smith, The spring transition in currents over the Oregon continental shelf, *J. Geophys. Res.*, *84*, 6995–7011, 1979.

Irish, J. D., CODE-2: Moored temperature and conductivity observations, in CODE-2: Moored Array and Large-Scale Data Report, *Tech. Rep. 85-35*, edited by R. Limeburner, pp. 165–178, Woods Hole Oceanogr. Inst., Woods Hole, Mass., 1985.

Kundu, P. K., J. A. Allen, and R. L. Smith, Modal decomposition of the velocity field near the Oregon coast, *J. Phys. Oceanogr.*, *5*, 683–704, 1975.

Lahey, J. F., R. A. Bryson, and E. W. Wahl, *Atlas of Five-Day Normal Sea-Level Pressure Charts for the Northern Hemisphere*, The University of Wisconsin Press, Madison, 1958.

Large, W. G., and S. Pond, Open ocean momentum flux measurements in moderate to strong winds, *J. Phys. Oceanogr.*, *11*, 324–336, 1981.

Lentz, S., A description of the 1981 and 1982 spring transitions over the northern California shelf, *J. Geophys. Res.*, this issue.

Strub, P. T., J. S. Allen, A. Huyer, R. L. Smith, and R. C. Beardsley, Seasonal cycles of currents, temperatures, winds, and sea level over the northeast Pacific continental shelf: 35°N to 48°N, *J. Geophys. Res.*, this issue.

Thomson, R. E., W. R. Crawford, H. J. Freeland, and W. S. Huggett, Low-pass filtered current meter records for the west coast of Vancouver Island: Coastal Oceanic Dynamics Experiment, 1979–81, *Can. Data Rep. Hydrogr. Ocean Sci. 40*, 102 pp., Inst. of Ocean Sci., Sidney, British Columbia, Canada, 1985.

Winant, C. D., and A. W. Bratkovich, CODE-1: Moored current observations, in CODE-1: Moored Array and Large-Scale Data Report, *Tech. Rep. 83-23*, edited by L. K. Rosenfeld, pp. 55–80, Woods Hole Oceanogr. Inst., Woods Hole, Mass., 1983.

Winant, C. D., U. Send, and S. J. Kentz, CODE-2: Moored current observations, in CODE-2: Moored Array and Large-Scale Data Report, *Tech. Rep. 85-35*, edited by R. Limeburner, pp. 73–108, Woods Hole Oceanogr. Inst., Woods Hole, Mass., 1985.

J. S. Allen, A. Huyer, R. L. Smith, and P. T. Strub, College of Oceanography, Oregon State University, Corvallis, OR 97331.

(Received April 28, 1986;
accepted July 1, 1986.)